IOP PUBLISHING JOURNAL OF PHYSICS D: APPLIED PHYSICS

J. Phys. D: Appl. Phys. **41** (2008) 205105 (6pp) doi:10.1088/0022-3727/41/20/205105

Epitaxial growth and luminescence properties of ZnO-based heterojunction light-emitting diode on Si(1 1 1) substrate by pulsed-laser deposition

Y W Zhang[1,4], X M Li[1,5], W D Yu[1,4], X D Gao[1], Y F Gu[1,4], C Yang[1,4], J L Zhao[2], X W Sun[2], S T Tan[2], J F Kong[3] and W Z Shen[3]

[1] State Key Laboratory of High Performance Ceramics and Superfine Microstructures, Shanghai Institute of Ceramics, Chinese Academy of Sciences, Shanghai 200050, People's Republic of China
[2] School of Electrical and Electronic Engineering, Nanyang Technological University, Nanyang Avenue, Singapore 639798, Singapore
[3] Laboratory of Condensed Matter Spectroscopy and Opto-Electronic Physics, Department of Physics, Shanghai Jiao Tong University, Shanghai 200030, People's Republic of China
[4] Graduate School of Chinese Academy of Sciences, Beijing 100039, People's Republic of China

E-mail: lixm@mail.sic.ac.cn

Received 23 July 2008, in final form 2 September 2008
Published 30 September 2008
Online at stacks.iop.org/JPhysD/41/205105

Abstract
An epitaxial ZnO heterojunction light-emitting diode with an n-ZnO/MgO/TiN/n^+-Si structure is produced by pulsed-laser deposition. By introducing a thin MgO/TiN buffer and a low temperature (LT) ZnO buffer, layer-by-layer growth of high quality ZnO epi-layer on Si(1 1 1) has been realized, which was confirmed by *in situ* reflection high-energy electron diffraction (RHEED), transmission electron microscopy, high-resolution x-ray diffraction, resonant Raman spectra and photoluminescence spectroscopy. Combining *in situ* RHEED with Phi-scan XRD analysis, the in-plane epitaxial growth of ZnO$[1\,1\,\bar{2}\,0]||$MgO$[1\,0\,\bar{1}]||$Si$[1\,0\,\bar{1}]$ has been demonstrated. The strong room temperature electroluminescence (EL) with a broad emission band ranging from 1.46 to 3.5 eV and centred at 2.31 eV could be observed from the diode under relative low injection current. Furthermore, the EL output light intensity is enhanced obviously by improving the ZnO crystal quality via inserting a ZnO LT buffer layer.

(Some figures in this article are in colour only in the electronic version)

1. Introduction

Zinc oxide is attracting considerable interest for optoelectronics applications because of its superior advantages over III-nitride semiconductors such as large exciton binding energy, high quality bulk substrates and ease of wet etching. The realization of blue/ultraviolet and white solid state light-emitting devices at room temperature (RT) is a worldwide pursuit for substituting the high-energy-cost light sources now used [1–8]. Recently, light-emitting diodes (LEDs) based on ZnO p–n homojunction have been achieved; however, low concentration and mobility of holes in p-type layers greatly limit their light-emitting efficiency [6–8]. As an alternative pathway, a number of studies on ZnO-based heterojunction LEDs have been reported, such as ZnO/Si, ZnO/GaN, ZnO/GaAs, ZnO/SiC, ZnO/$SrCu_2O_2$ [4, 9–16]. Among these materials, silicon has prominent merits of realizing lower driving voltage of LED and lower cost of device due to well-developed Si integrated technology. As is well known, a high crystal quality ZnO layer is preferred for fabricating LEDs. However, the large lattice mismatch between ZnO and Si (−15.4%) will obstruct the acquirement of a high crystal quality ZnO layer on the Si substrate. Recently,

[5] Author to whom any correspondence should be addressed.

buffer layer technology has been developed to improve the epitaxial quality of the ZnO film on the Si substrate, such as ZnO/AlN/Si, ZnO/MgO/Mg/Si, ZnO/MgO/TiN/Si [17–19]. Moreover, these dielectric buffer layers can also act as carrier blockers for the ZnO/Si heterostructred LED [15]. In our previous work, epitaxial n-ZnO/MgO/TiN/n^+-Si heterostructured LEDs have been reported [20]. MgO/TiN buffer layers were deposited by pulsed-laser deposition (PLD) while a ZnO epilayer was grown by metal-organic chemical-vapour deposition (MOCVD). A strong wide electroluminescence (EL) band in epitaxial ZnO can be observed from the diode.

In this paper, we will report systematical studies on the structural and optical properties, as well as LED applications of the n-ZnO/MgO/TiN/n^+-Si heterostructure, which was entirely fabricated by PLD. In order to improve the crystal quality and reduce deep-level (DL) defects in the ZnO epi-layer, a low temperature (LT) ZnO buffer layer was employed in the growth process of ZnO epitaxial on the MgO/TiN/Si(1 1 1) substrate. Meanwhile we have comparatively investigated the growth process, crystal quality and luminescence performance of n-ZnO/MgO/TiN/n^+-Si heterojunctions with or without a LT ZnO buffer layer. It is found that no significant DLEs appear in photoluminescence (PL) spectroscopy, and the EL output light intensity is enhanced obviously by improving the ZnO crystal quality via employing a LT ZnO buffer layer.

2. Experimental details

n-ZnO/MgO/TiN/n^+-Si samples were fabricated by PLD using a KrF excimer laser ($\lambda = 248$ nm, repetition rates of 5 Hz). The focused laser energy density was set at 7 J cm^{-2} and the target–substrate distance was optimized to 70 mm. Commercial n^+-Si(1 1 1) (resistivity $\sim 10^{-3}\ \Omega$ cm) wafers were cleaned for 3 min in a mixed solution of HF : distilled water : ethanol in a volume ratio of 1 : 1 : 10 to remove the surface native oxide layer. The growth chamber was evacuated to the order of 10^{-5} Pa; a thin layer of TiN ($\sim$3 nm) was then deposited on Si(1 1 1) at 600 °C, which can have the benefit of relaxing the mismatch between MgO and Si and avoid the oxidation of the Si surface during the subsequent MgO growth [16]. Then a pure O_2 gas was introduced into the chamber and the pressure during subsequent deposition following was maintained at 1×10^{-2} Pa, the MgO layer ($\sim$25 nm) was *in situ* grown at 600 °C and then conventional two-step growth of ZnO was performed (sample A) as follows: first a LT ZnO buffer layer ($\sim$40 nm) was grown at 500 °C; second the LT buffer was *in situ* annealed at 750 °C for 15 min; finally a high temperature (HT) ZnO layer ($\sim$160 nm) was subsequently grown at 700 °C. For comparison a ZnO film ($\sim$200 nm) without a LT buffer layer was grown on MgO/TiN/Si directly at 700 °C (sample B). To obtain n-ZnO/MgO/TiN/n^+-Si based LEDs, an Au electrode was deposited onto ZnO and the backside of the Si wafer by direct-current magnetron sputtering, where the electrode on ZnO was patterned into 1 mm diameter via shadow mask.

The in-plane epitaxial relationship, surface morphology evolution and crystallinity were *in situ* monitored by reflection high-energy electron diffraction (RHEED). The crystallinity of te ZnO film was characterized by high-resolution x-ray diffraction (HRXRD) on a Philips double-axis high-resolution diffractometer at 45 kV and 40 mA for both the rocking curve measurement and in-plane phi-scan using copper Kα radiation. A Philips CM200 field emission gun transmission electron microscope (TEM), operating at 200 kV, was used for cross-sectional microstructure observation. The resonant Raman scattering (RRS) and PL spectroscopy measurements were performed at the same installation (Jobin Yvon LabRAM HR 800UV), excited by the 325 nm line of a 5 mW He–Cd laser and measured at RT. I–V characteristics of the heterojunction were investigated using a HP 4156A semiconductor parameter analyzer, and the EL signal was collected using optical fibre, split through the monochromator and detected by a photomultiplier.

3. Results and discussion

In-plane epitaxial relations can be inferred from RHEED patterns (figure 1). The RHEED pattern from the ZnO film on buffer layered Si (figure 1(*e*)) is sharply streaky, implying the realization of layer-by-layer epitaxial growth. The streak pattern can be observed six times by rotating the film around its normal for 360°. The six-fold symmetry indicates in-plane alignment of epitaxial ZnO$[1\,1\,\bar{2}\,0]||$MgO$[1\,0\,\bar{1}]||$Si$[1\,0\,\bar{1}]$. Then we describe the detailed growth processes of the ZnO epi-layer based on *in situ* RHEED observations. When the deposition of TiN starts, the sharp streaky pattern of the Si(1 1 1) substrate (figure 1(*a*)) vanishes quickly and no RHEED signal is found (figure 1(*b*)) in place of the substrate, perhaps due to the special state of TiN_xO_y, which behaves like a mixture of amorphous structure and crystalline structure while still maintaining the cubic structure of TiN [21]. This phenomenon is favourable for subsequent layer-by-layer growth of MgO and ZnO. The six-fold symmetrical streaky pattern (figure 1(*c*)) indicates that rock-salt MgO with a flat surface grows along the [1 1 1] crystal orientation with the following epitaxial relationship of MgO$[1\,0\,\bar{1}]||$Si$[1\,0\,\bar{1}]$ (in plane). LT ZnO growth is then carried out after MgO buffer deposition. Spotty patterns of ZnO (figure 1(*d*)) immediately appear superimposing on the MgO patterns. During the growth process of the LT ZnO buffer layer, the spotty patterns remain. When the temperature ramps up to 750 °C after LT ZnO buffer deposition, the RHEED pattern becomes streaky gradually. After 15 min annealing at 750 °C, sharp streaky RHEED patterns of ZnO appear (figure 1(*e*)), which marks the completion of the buffer growth process. According to the RHEED patterns, the epitaxial relationship is determined as ZnO$[1\,1\,\bar{2}\,0]||$MgO$[1\,0\,\bar{1}]$ and ZnO$[1\,0\,\bar{1}\,0]||$MgO$[1\,1\,\bar{2}]$. The growth of the ZnO epi-layer then restarts at 700 °C. After the epitaxial growth at this temperature for 1 h, the sample still maintains the streaky and spots RHEED patterns (figure 1(*f*)). Whereas only spotty RHEED patterns (figure 1(*g*)) were observed in the ZnO films without a ZnO LT buffer layer (sample B), demonstrating island growth mode and rather poor crystallinity, which was further confirmed by HRXRD and RRS. Here, we have shown how to achieve layer-by-layer growth of ZnO film on Si(1 1 1), and in which the key step is employing MgO/TiN buffer layers and LT ZnO buffer layer.

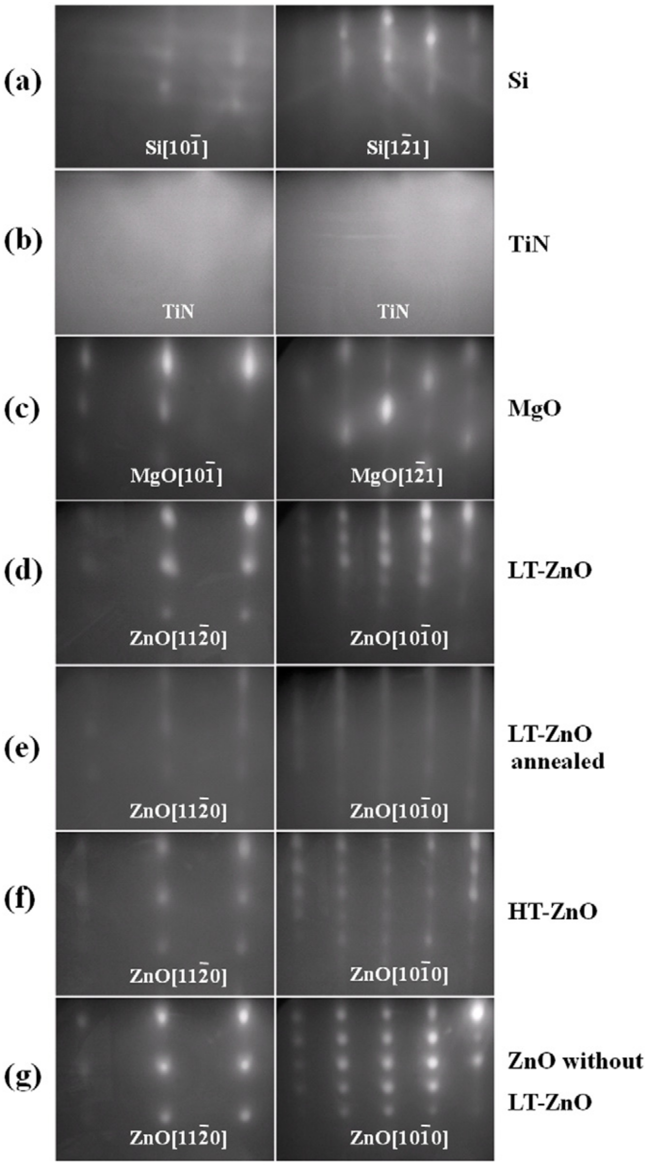

Figure 1. Evolution of RHEED patterns during ZnO epitaxy growth. Bare Si(1 1 1) substrate (*a*), TiN buffer layer (*b*), streaky and spots of MgO buffer layer (*c*), as-grown LT ZnO layer at 500 °C (*d*), LT ZnO layer annealed at 750 °C for 15 min (*e*), ZnO epi-layer at 700 °C after 1 h growth (*f*) on the annealed LT buffer (sample A). ZnO epi-layer at 700 °C after 1.5 h growth without LT ZnO buffer layer(sample B) (*g*).

A cross-sectional HRTEM study with different magnifications is carried out to determine the interface microstructure of the ZnO/MgO/TiN/Si system (sample A). In figure 2(*a*), a relatively smooth interface can be observed over the imaged region. The thickness of each layer (figure 2(*b*)) (denoted by arrows) is about 3 nm, 25 nm, 200 nm, respectively. We consider that there is a mixed structure layer of TiN_xO_y between MgO and Si (figure 2(*c*)) by utilizing a TiN target, consistent with the fact that no TiN signal appeared in RHEED patterns (figure 1(*b*)). It should be noted that the interface between ZnO and MgO is atomically sharp without any indications of inter-diffusion or an amorphous structure (figure 2(*d*)). The continuous crystalline feature of this interface layer suggests that layer-by-layer ZnO growth is formed, which is consistent with the results of streaky RHEED patterns in figure 1(*e*).

The crystallinity of ZnO films deposited on MgO/TiN buffer layers with or without ZnO LT buffer was comparatively investigated by HRXRD (figure 3). In the $\theta/2\theta$ scan curve, there is only one obvious diffraction peak indexed as the hexagonal ZnO(0 0 0 2), indicating strictly *c*-axis oriented growth of the ZnO films. The full width at half maximum (FWHM) of the ω-scan rocking curve [ZnO (0 0 0 2)] of sample A and sample B are 1.0° and 1.9°, respectively (inset of figure 3), and the less FWHM of sample A demonstrates rather better crystallinity of the ZnO film with LT buffer. Phi-scan was employed to further analyse the in-plane orientation of the ZnO film relative to the Si substrate, as shown in figure 3(*c*). Six sharp Phi-scan peaks of the ZnO (1 0 $\bar{1}$ 1) at 60° intervals confirm that the epitaxial ZnO exhibits a single-domain wurtzite structure with hexagonal symmetry. Moreover, Phi-scan also indicates that the surface lattices of ZnO (0 0 0 2) and Si (1 1 1) are exactly overlapped without any rotation, with an in-plane epitaxial relationship as ZnO[1 0 $\bar{1}$ 0]||Si[1 1 $\bar{2}$] consistent with the results inferred from RHEED patterns.

The RRS is a powerful tool to determine the quality of the *c*-axis textured ZnO films [22]. It is worth noting that the frequency of the LO phonon mode of the Sample A in figure 4 is 568 cm^{-1}, which coincides with that of the A_1LO mode of the ZnO single crystal, indicating the high *c*-axis orientation of the epitaxial ZnO films with LT buffer. Sample B also exhibits *c*-axis texture as revealed by XRD (figure 3(*b*)). However in its RRS, ω_{LO} is 5 cm^{-1} higher than ω_{A1LO}, implying that the crystalline grains are tilted to the *c* axis and leading to the mix-mode character of the RRS LO phonon mode [22]. In figure 4 it is also notable that the ratio of Raman intensity of second LO phonon and first LO phonon (I_{2LO}/I_{LO}) of sample A is almost twice larger than that of sample B, revealing larger electron–LO phonon coupling of epitaxial ZnO films with LT buffer [22]. As known, the second-order structures are very sensitive to atomic scale disorder, and thus the I_{2LO}/I_{LO} ratio will be increased due to improvement in the ZnO films crystal quality resulting from inserting LT ZnO buffer.

The current–voltage (I–V) curves of the heterojunction units with or without LT ZnO buffer are shown in figure 5. Both samples show the typical characteristics of a back-to-back diode, which has been discussed in our previous study [20]. Ohmic contact was confirmed for Au/n-ZnO, as shown in the inset of figure 5. The MgO layer acts as a double Schottky barrier for both n-ZnO and n^+-Si and the junction can be considered as a series of two back-to-back Schottky diodes. Meanwhile it is interesting that the rectifying characteristic of the sample A is better than that observed in the sample B. Considering the structural analysis above, it is possible that the LT buffer process can effectively reduce donor-like defects which would provide the recombination tunnelling path and worsen the rectifying characteristic [10].

The samples are also proven to have a good optical quality by PL measurement at RT (figure 6). In our previous study, a strong wide visible emission in epitaxial ZnO grown by MOCVD can be observed in PL measurements [20], whereas no significant DLEs are detected in this work which implies

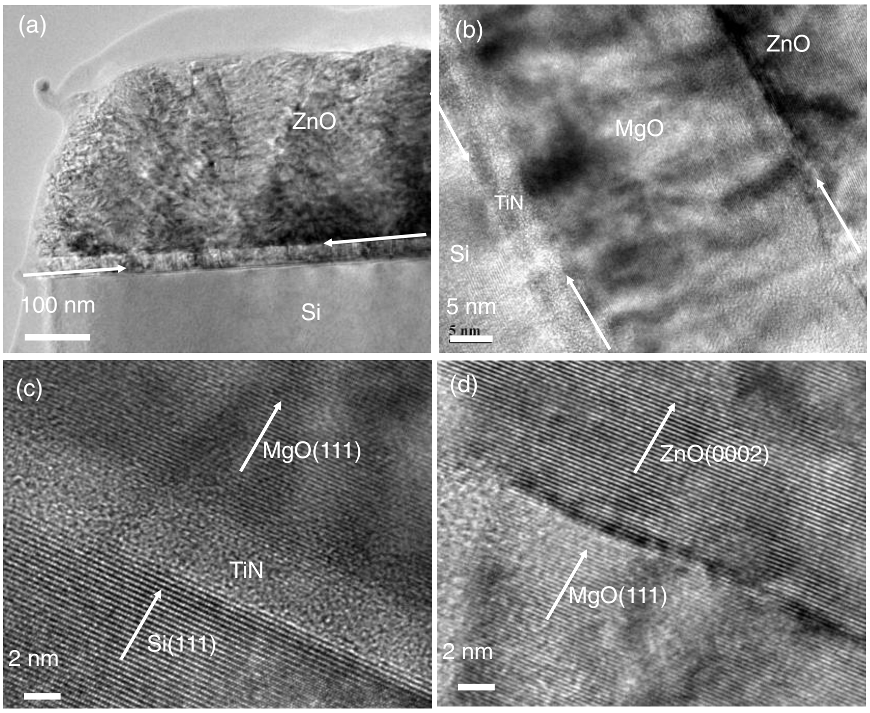

Figure 2. HRTEM micrograph shows the cross-sectional details of the ZnO/MgO/TiN/Si interface region: the panorama micrograph (*a*), the two interfaces of ZnO/MgO and MgO/TiN/Si (*b*), magnified image of MgO/TiN/Si (*c*), magnified image of ZnO/MgO (*d*).

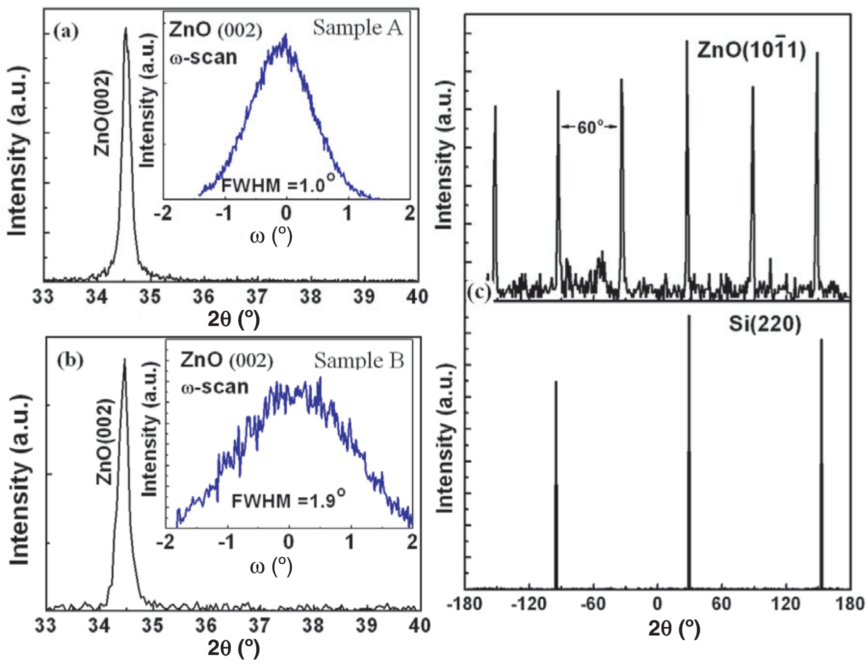

Figure 3. XRD spectra of the epitaxial ZnO samples on MgO/TiN buffered Si (1 1 1): $\theta/2\theta$ scan for sample A (*a*) and sample B (*b*), Phi-scans for ZnO (1 0 $\bar{1}$ 1) and Si (2 2 0) (*c*). The insets in (*a*) and (*b*) show the ω-scan rocking curves of ZnO (0 0 0 2) for samples A and B, respectively.

much lower DL defect concentration of the samples due to good crystal quality as confirmed by the structural analysis above. Moreover, a strong near-band-edge (NBE) emission is observed at 3.30 eV with a FWHM of about 95 meV for the both samples, which is comparable to those of ZnO bulk crystal [23], and high quality ZnO films on sapphire [24] and $ScAlMgO_4$ [6], indicating good optical quality of epitaxial ZnO films produced by PLD on the MgO/TiN buffer layer.

Strong EL of the ZnO-based heterojunction LED can be observed at RT under injection current of 80 mA (figure 6). The EL emission with yellowish-white light is so obvious that it can be clearly seen by the naked eye at RT, when a positive voltage is applied on the top electrode of Si substrates (forward bias). However, no emission is observed under reverse bias. The EL spectrum exhibits a broad band from 1.46 to 3.50 eV with the peak at 2.31 eV. The EL mechanism

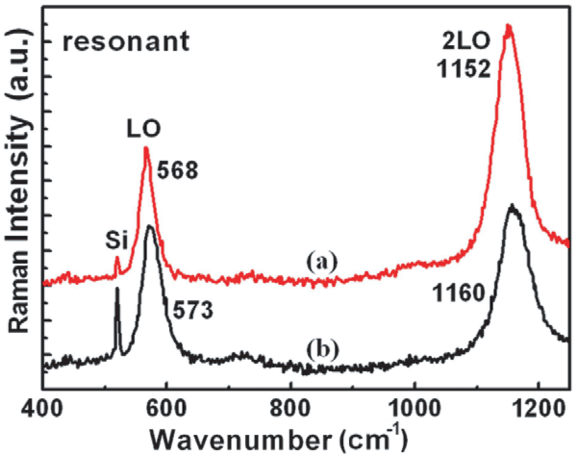

Figure 4. Resonant Raman spectra of the epitaxial ZnO films with LT ZnO buffer (sample A) (a) and without LT ZnO buffer (sample B) (b). The vibrational mode located at 520 cm^{-1} originates from the Si substrate.

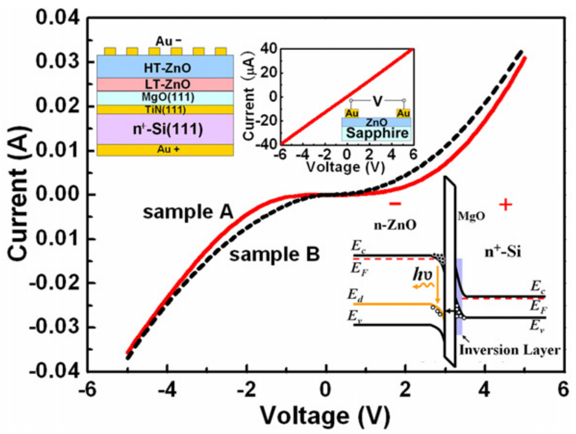

Figure 5. Current–voltage characteristic of the n-ZnO/MgO/TiN/n^+-Si diode for sample A (solid line) and sample B (dashed line). The top left inset illustrates the diode structure of sample A, the top middle inset shows the ohmic contact between Au and n-ZnO and the bottom right inset shows the energy band diagram of the diode under positive bias at Si side.

is similar to that discussed in our previous work [20]. The energy band diagram of the diode under positive bias is shown in figure 5. Since the TiN layer is very thin, we neglected it in the diagram. When a positive bias is applied on the Si diode, the energy bands of Si near the interface bend upwards, inducing an inversion layer with hole accumulation. Under the electric field the holes accumulated at the Si/MgO interface is swept to the ZnO side through the MgO layer by tunnelling. Moreover, the electrons are injected into ZnO from Au under bias and accumulate near the ZnO/MgO interface due to blocking of MgO barrier. Consequently, the EL originates from the recombination between the injected electrons and holes via DL states at ZnO layer near the ZnO/MgO interface. It is also notable that the output light intensity of sample A is almost twice larger than that of sample B, revealing lower nonradiative centre concentration of epitaxial ZnO films with LT buffer due to better crystal quality [7]. Moreover the 80 mA injection current is much lower than that (192 mA) of

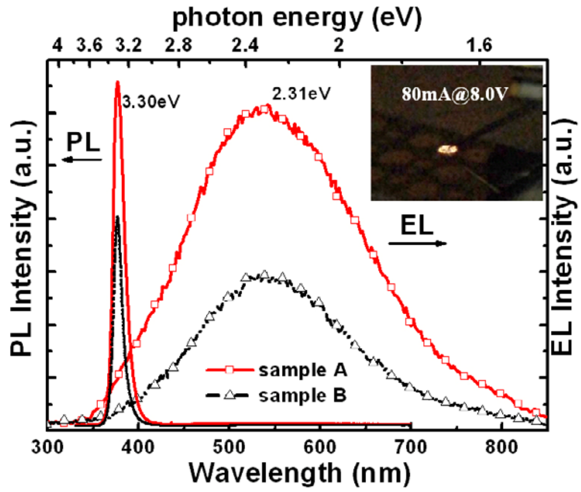

Figure 6. RT PL spectra from the ZnO films of sample A (solid line) and sample B (dashed line) on MgO/TiN/Si. RT EL spectra from the n-ZnO/MgO/TiN/n^+-Si LED for sample A (solid line with symbol) and sample B (dashed line with symbol). Inset shows the photograph of the emitting LED (sample A) at 80 mA and 8.0 V.

the heterostructured LED reported in our previous work with comparable output light intensity (sample A) [20]. This result is consistent with the above analysis that less nonradiative centres related defects exist in high quality epitaxial ZnO by the LT buffer process. However, compared with the PL spectrum, the intensity of NBE emission is much weaker and the DL emission appears prominently in the EL spectrum. This distinction gives strong evidence for the presence of DL defects in the ZnO layer near the ZnO/MgO interface, which is mainly induced by the mismatch between ZnO and MgO [16]. So how to further reduce the defects induced by the mismatch at the interface is the key to realizing a high performance ZnO-based EL device integrated on Si.

4. Conclusions

In summary, an epitaxial n-ZnO/MgO/TiN/n^+-Si heterostructured LED was entirely fabricated by PLD. High quality epitaxial ZnO was achieved on the Si(1 1 1) substrate by introducing the MgO/TiN buffer layers and the ZnO LT buffer layer. As a result, the in-plane relationship is shown to be ZnO$[1\,1\,\bar{2}\,0]\|$MgO$[1\,0\,\bar{1}]\|$Si$[1\,0\,\bar{1}]$, which was confirmed by RHEED patterns and Phi-scan. The distinct RT EL with a broad emission band ranging from 1.46 to 3.5 eV could be observed from the diode under relative low injection current. Meanwhile, the output light intensity is enhanced evidently by using the ZnO LT buffer layer, which is also useful to realizing ZnO layer-by-layer epitaxy growth mode and improving the crystal quality of the ZnO films. These achievements indicate that the all-epitaxy technology may be a good route to obtain low-cost and high performance ZnO-based LED integrated on Si.

Acknowledgments

This work was supported by the ministry of Science and Technology of People's Republic of China through the 973 National Nature Science Foundation (No 2002CB613306). The authors would like to acknowledge the financial support from Singapore Agency for Science, Technology and Research (A*STAR) SERC Public Sector Fund (No 0421010010) and Inter-RI project (No 0521260095).

References

[1] Service R F 1997 *Science* **276** 895
[2] Sun X W and Kwok H S 1999 *J. Appl. Phys.* **86** 408
[3] Ryu Y R, Lubguban J A, Lee T S, White H W, Jeong T S, Youn C J and Kim B J 2007 *Appl. Phys. Lett.* **90** 131115
[4] Özgür Ü, Alivov Y I, Liu C, Teke A, Reshchikov M A, Doğan S, Avrutin V, Cho S J and Morkoç H 2005 *J. Appl. Phys.* **98** 041301
[5] Look D C 2007 *Proc. SPIE* **6474** 647402
[6] Tsukazaki A *et al* 2005 *Nature Mater.* **4** 42
[7] Liu W *et al* 2006 *Appl. Phys. Lett.* **88** 092101
[8] Lin S S, Ye Z Z, Lu J G, He H P, Chen L X, Gu X Q, Huang J Y, Zhu L P and Zhao B H 2008 *J. Phys. D: Appl. Phys.* **41** 155114
[9] Chen P, Ma X and Yang D 2007 *J. Appl. Phys.* **101** 053103
[10] Ye J D, Gu S L, Zhu S M, Liu W, Liu S M, Zhang R, Shi Y and Zheng Y D 2006 *Appl. Phys. Lett.* **88** 182112
[11] Chen C P, Ke M Y, Liu C C, Chang Y J, Yang F H and Huang J J 2007 *Appl. Phys. Lett.* **91** 091107
[12] Du G T, Liu W F, Bian J M, Hu L Z, Liang H W, Wang X S, Liu A M and Yang T P 2006 *Appl. Phys. Lett.* **89** 052113
[13] Alivov Y I, Kalinina E V, Cherenkov A E, Look D C, Ataev B M, Omaev A K, Chukichev M V and Bagnall D M 2003 *Appl. Phys. Lett.* **83** 4719
[14] Yuen C, Yu S F, Lau S P, Rusli and Chen T P 2005 *Appl. Phys. Lett.* **86** 241111
[15] Zhao J L, Sun X W, Tan S T, Lo G Q, Kwong D L and Cen Z H 2007 *Appl. Phys. Lett.* **91** 263501
[16] Sun J W, Lu Y M, Liu Y C, Shen D Z, Zhang Z Z, Li B H, Zhang J Y, Yao B, Zhao D X and Fan X W 2008 *J. Phys. D: Appl. Phys.* **41** 155103
[17] Wang X N *et al* 2007 *Appl. Phys. Lett.* **90** 151912
[18] Jiang F, Zheng C, Wang L, Fang W, Pu Y and Dai J 2007 *J. Luminesc.* **122–123** 905
[19] Jin C M, Narayana R, Tiwarib A, Zhou H H, Kvit A and Narayan J 2005 *Mater. Sci. Eng.* B **117** 348
[20] Sun X W, Zhao J L, Tan S T, Tan L H, Tung C H, Lo G Q, Kwong D L, Zhang Y W, Li X M and Teo K L 2008 *Appl. Phys. Lett.* **92** 111113
[21] Vaz F, Cerqueira P, Rebouta L, Nascimento S M C, Alves E, Goudeau Ph, Riviere J P, Pischow K and de Rijk J 2004 *Thin Solid Films* **447–448** 449
[22] Du C L, Gu Z B, You Y M, Kasim J, Yu T, Shen Z X, Ni Z H, Ma Y, Cheng G X and Chen Y F 2008 *J. Appl. Phys.* **103** 023521
[23] Harada Y and Hashimoto S 2003 *Phys. Rev.* B **68** 045421
[24] Chen Y F, Bagnall D M, Koh H J, Park K T, Hiraga K, Zhu Z and Yao T 1998 *J. Appl. Phys.* **84** 3912